International Journal of Minerals, Metallurgy and Materials
Volume 21, Number 4, April 2014, Page 345
DOI: 10.1007/s12613-014-0915-8

Dissolution and diffusion of TiO_2 in the CaO-Al_2O_3-SiO_2 slag

Zhong-shan Ren[1,2], *Xiao-jun Hu*[1], *Xin-mei Hou*[2], *Xiang-xin Xue*[3], *and Kuo-chih Chou*[1,2]

1) State Key Laboratory of Advanced Metallurgy, University of Science and Technology Beijing, Beijing 100083, China;
2) School of Metallurgical and Ecological Engineering, University of Science and Technology Beijing, Beijing 100083, China;
3) School of Materials and Metallurgy, Northeastern University, Shenyang 110006, China
(Received: 17 October 2013; revised: 10 November 2013; accepted: 13 November 2013)

Abstract: The dissolution of TiO_2 in the $CaO–Al_2O_3–SiO_2$ slag under static conditions was studied in the temperature range from 1643 K to 1703 K. After TiO_2 dissolved, the microstructure of the interface between TiO_2 and the slag was observed by scanning electron microscopy, and the concentration profiles of Ti^{4+} and other ions across the TiO_2/slag interfaces were analyzed by energy-dispersive X-ray spectroscopy. On the basis of these results, the dissolution behavior of TiO_2 was evaluated, and the diffusivity of Ti^{4+} in the bulk slag was estimated. According to the Stokes–Einstein relation, the viscosity calculated by a previously reported model gave a diffusivity of Ti^{4+} ions greater than that estimated by the concentration profiles of Ti^{4+} ions. The mechanism of TiO_2 dissolution in the $CaO–Al_2O_3–SiO_2$ slag is discussed in detail.

Keywords: slags; titanium dioxide; dissolution; diffusion; interface

1. Introduction

In secondary steelmaking, the molten slag plays a substantial role in improving the quality of the steel because it can absorb S, P, oxide inclusions, and other detrimental impurities via reactions between the slag and metal. In the case of titanium alloys or Ti-killed steel, Ti remaining in the liquid steel can combine with carbon, nitrogen, or oxygen to form TiN, TiC, Ti(C, N), TiO_2, and Ti-bearing composite inclusions [1–4], which would adversely affect the quality of the steel. Hence, the possibility of dissolving Ti-bearing inclusions has attracted widespread interest. However, in reactions between the slag and metal during metallurgical processes, the diffusivities of ions in the liquid metal are greater than the diffusivities of ions in the molten slag, and reactions between the slag and metal are therefore limited by the diffusion in the slag phase [5]. Consequently, investigations on the dissolution and diffusion behaviors of oxide inclusions in the molten slag are urgently needed.

Substantial research has been devoted to studying the dissolution of other oxides [6–9], such as MgO, CaO, or Al_2O_3; however, the literature contains few reports related to the dissolution of TiO_2 or Ti-bearing composite inclusions in molten slags. Wang *et al.* [10] studied the dissolution mechanism of synthesized Al_2TiO_5 inclusions in molten $CaO–Al_2O_3–SiO_2$ slags at 1823 K. In the early stage, the dissolution rate of Al_2TiO_5 inclusions was greater than the diffusion rate of the liquid product. As the dissolution time increased, the diffusion of the liquid phase became the rate-determining step, and the dissolution rate of Al_2TiO_5 equaled the diffusion rate of the liquid product at a later stage. During the dissolution process, the typical dissolution product was $CaTiO_3$. Following this idea, we here report the results of our investigation into the dissolution and diffusion of TiO_2 in $CaO–Al_2O_3–SiO_2$ slags under static conditions. The interface between TiO_2 and the slag was observed and analyzed by scanning electron microscopy (SEM) and energy-dispersive X-ray spectroscopy (EDS). The dissolution mechanism and diffusion kinetics are also discussed.

2. Experimental

2.1. Sample preparation

The materials used for the experiment were analytical

Corresponding author: Xiao-jun Hu E-mail: huxiaojun@ustb.edu.cn

reagent grade SiO_2, Al_2O_3, TiO_2, and $CaCO_3$ powders, all of which were calcined at 1273 K for 6 h in a muffle furnace to decompose any carbonates or hydroxides before use. TiO_2 disks (10 mm o.d. and 5 mm height) were prepared via the following procedure. The powders of TiO_2 charged in a stainless steel mold were compacted under a pressure of approximately 500 MPa for 3 min and then sintered at 1773 K for 12 h under an air atmosphere. The slag compositions used in the present study are listed in Table 1. According to the compositions shown in Table 1, the oxides were precisely weighed and premixed in an agate mortar. The mixtures charged in an alumina crucible (60 mm in outer diameter, 55 mm in inside diameter, and 80 mm in height) were premelted at 1773 K. After 1 h, the melts were quenched in an iron plate, crushed, and then stored in a desiccator.

Table 1. Initial chemical compositions of slags wt%

Slag No.	CaO	Al_2O_3	SiO_2	Basicity CaO/SiO_2
A	40.00	20.0	40.00	1.0
B	42.50	15.0	42.50	1.0
C	37.50	25.0	37.50	1.0
D	35.56	20.0	44.44	0.8
E	43.64	20.0	36.36	1.2

2.2. Experimental procedure

One side of a TiO_2 disk was ground and mechanically polished, and the disk was subsequently placed into an alumina crucible (16 mm in outer diameter, 13 mm in inside diameter, and 45 mm in height). After that, approximately 4 g of the slag was placed over the TiO_2 disk in each experiment; the height of the molten slag was approximately 12 mm at the experimental temperature. Because of the greater density of TiO_2 compared to that of the molten slag, local convection was avoided. The schematic illustration of the experimental setup used in the present work is presented in Fig. 1. The furnace was heated by six $MoSi_2$ elements, and the temperature was measured by a Pt–6%Rh/Pt–30%Rh (type B) thermocouple in an alumina sheath; the temperature was kept constant within ±2 K. When the furnace was heated to the desired temperature at a rate of 5 K/min, the alumina crucible, along with a graphite crucible, was gradually placed in the uniform temperature zone of the $MoSi_2$ furnace and rested on an alumina platform. After the required reaction time, the alumina crucible with its contents was raised rapidly and quenched in air. Notably, the preheating time of the alumina crucible in each run was constant. The dissolution experiments for slag A were conducted at 1643, 1673, and 1703 K, and the dissolution of TiO_2 in other slags was conducted only at 1673 K for 4 min.

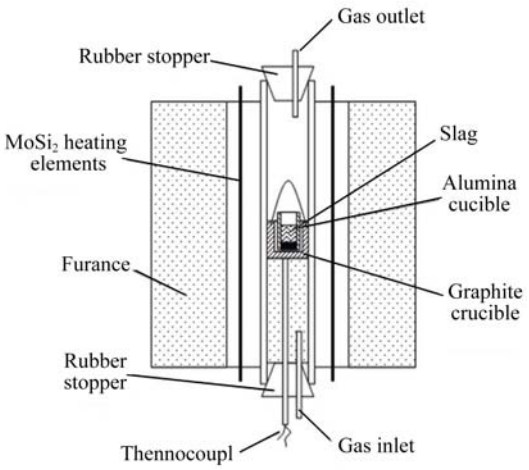

Fig. 1. Schematic illustration of the experimental setup.

After cooling, the specimens were embedded in cold-setting epoxy resin and cut perpendicular to the bottom of the alumina crucible with a diamond saw. The sectioned surface was polished with different mesh number SiC polishing papers and then ultrasonically cleaned in ethyl alcohol. The microstructure of the specimens after they were carbon coated was observed by scanning electron microscopy (SEM, ZEISS EVO–18), and the concentration distributions of different elements along the direction perpendicular to the TiO_2/slag interface were analyzed by EDS.

3. Results

Fig. 2 shows the SEM images of interfaces between slag A and TiO_2 after dissolution for 4 min at 1643, 1673, and 1703 K. The phase on the left side is TiO_2, whereas the bulk slag is on the right side. As evident in the figure, numerous crystal phases between the slag and TiO_2 were present in the samples at 1673 and 1703 K. This phase likely precipitated from the slag during quenching because the cooling rate was insufficient. However, in the case of the specimen at 1643 K, the dissolution of TiO_2 was not obvious and the crystallized phase was not formed because of the low temperature. To identify the product phase, we performed numerous EDS analyses. For example, some results are shown in the SEM images of interfaces between slag E and TiO_2 after dissolution for 4 min at 1673 K (Fig. 3). The crystal phase, although it assumed different forms, contained only $CaTiO_3$, and the same result was reported by Wang *et al.* [10].

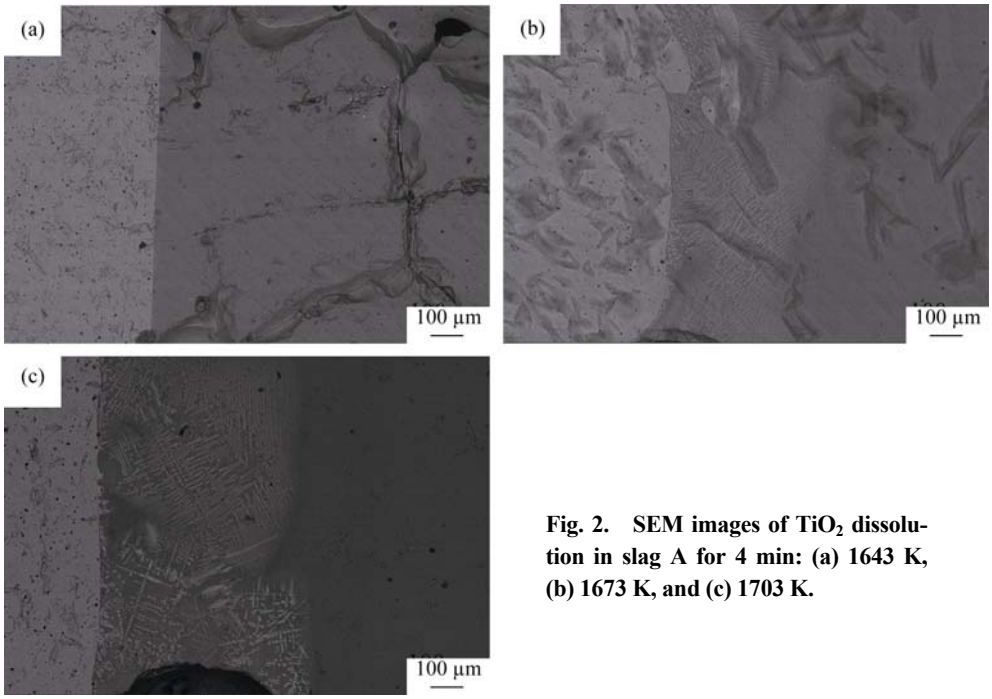

Fig. 2. SEM images of TiO_2 dissolution in slag A for 4 min: (a) 1643 K, (b) 1673 K, and (c) 1703 K.

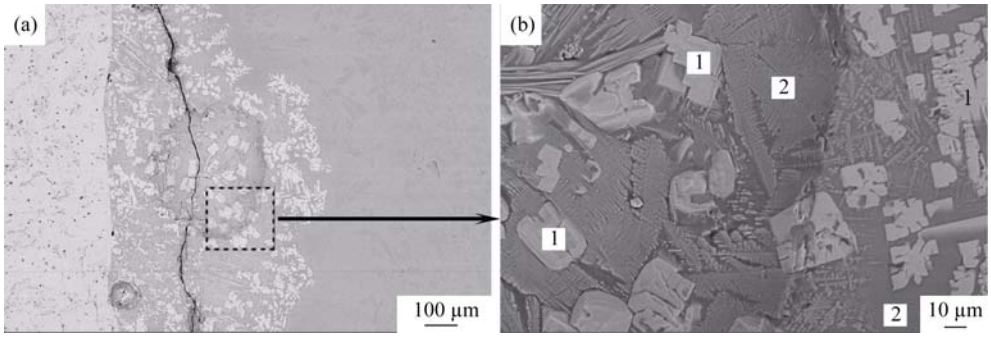

Fig. 3. SEM images of TiO_2 dissolution in slag E for 4 min at 1673 K: 1—$CaTiO_3$; 2—TiO_2-bearing slag.

Because the bulk slag was free of TiO_2, the concentration of TiO_2 would vary across interfaces between TiO_2 and the slag during the dissolution process. Therefore, the concentration profile of TiO_2 can be used to reveal the dissolution behavior. Fig. 4 shows the concentration profiles of main elements in the system analyzed by EDS at different positions across the interfaces. Notably, the concentration of O ions was calculated on the basis of the concentrations of other elements; e.g., one Al atom carries 1.5 O atoms, and one Si or Ti carries two O atoms. In Fig. 4, we observed a diffusion process of Ti^{4+} ions in the slag along with the dissolution process of TiO_2; the concentration change caused by the diffusion is shown in the dotted box. Using the concentration profiles, we determined the thickness of the dissolution and diffusion layers (defined in section 4.3) by measuring relative distance between the position where the concentration of Si^{4+} or Al^{3+} ions becomes zero and the position where the concentration of Ti^{4+} ions becomes zero, as marked in Fig. 4.

4. Discussion

4.1. Growth of the dissolution and diffusion layers

From the concentration profiles of the main elements, we measured the thickness of the dissolution and diffusion layers (*i.e.*, the D–D layer) in Fig. 4. The effects of temperature, dissolution time, Al_2O_3 content, and basicity on the thickness of the D–D layer are shown in Fig. 5. As shown in Fig. 5(a), the thickness of the D–D layer increased with increasing temperature. The effect of the dissolution time was similar to that of temperature; however, the growth rate in the later stage was smaller than that in the earlier stage. In the earlier stage, the dissolution of TiO_2 into the slag was very rapid, and the thickness of the D–D layer therefore rapidly increased. As the dissolution time was extended, the dissolution became difficult when the TiO_2 content in the

molten slag was very high. However, because of the difference in Ti^{4+} concentration, Ti^{4+} in the dissolution layer would diffuse toward the bulk slag, and the diffusion would become the rate-controlling step. Consequently, the thickness of the D–D layer grew slowly during the later stage. As shown in Fig. 5(c) and Fig. 5(d), as the content of Al_2O_3 in the slag increased, the thickness of the D–D layer continuously decreased. However, with increasing basicity, the thickness of the D–D layer first decreased and then increased. In general, Al_2O_3 acts as an acidic oxide and Al^{3+}

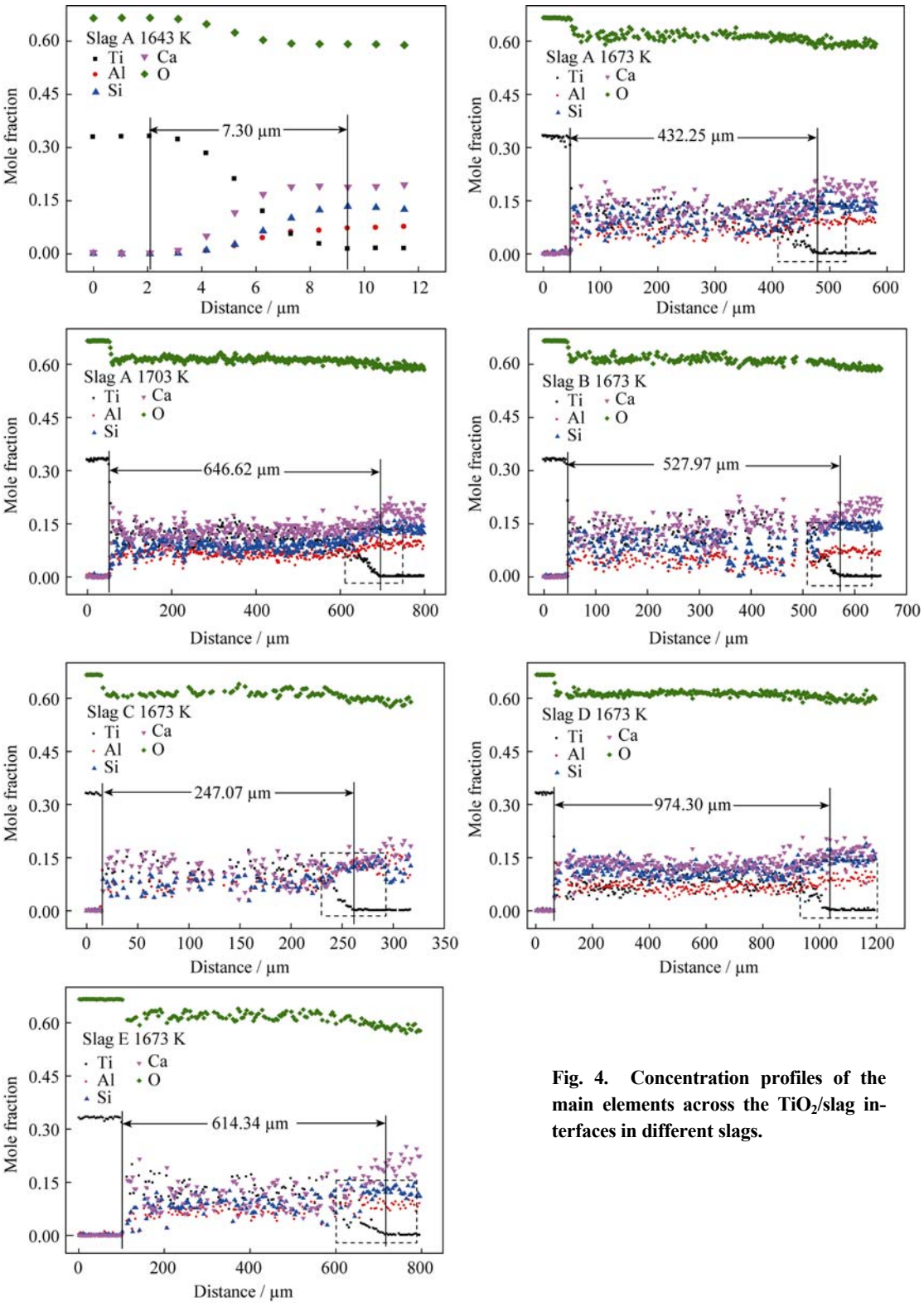

Fig. 4. Concentration profiles of the main elements across the TiO_2/slag interfaces in different slags.

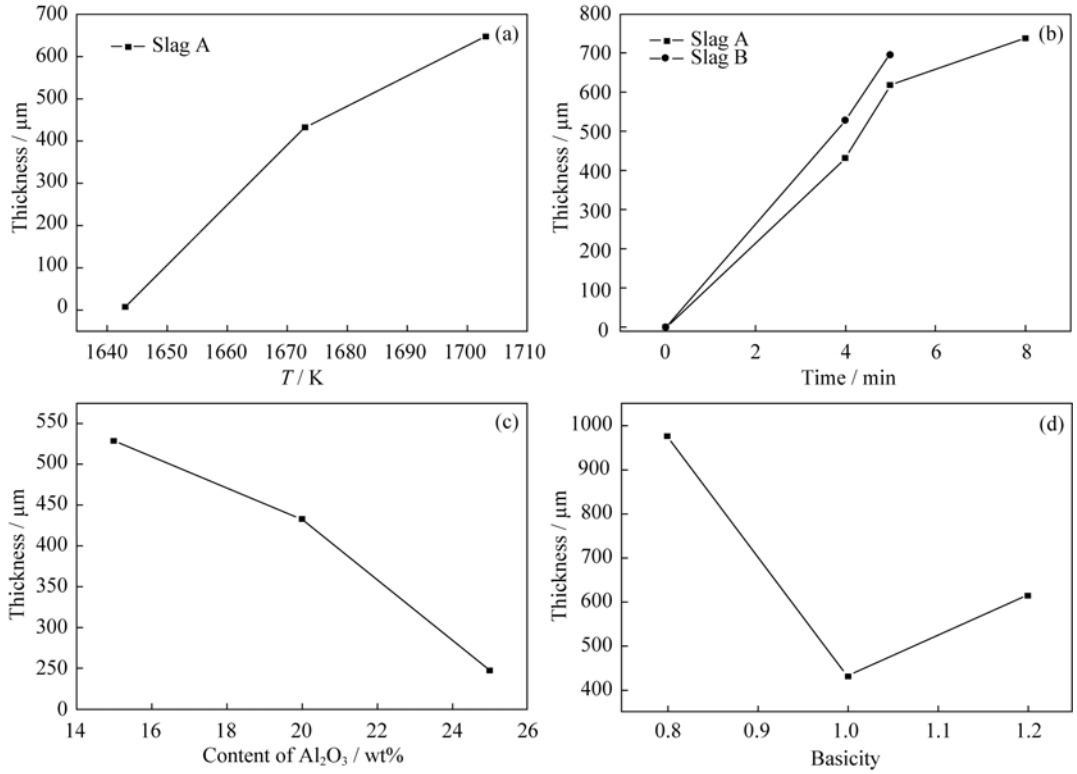

Fig. 5. Thickness of the D–D layer plotted as a function of (a) temperature, (b) dissolution time, (c) Al_2O_3 content, and (d) basicity.

ions can also form a tetrahedrally coordinated AlO_4^{5-} structure, similar to Si^{4+} ions, which can enhance the polymerization degree of the molten slag. Therefore, a greater concentration of Al_2O_3 in the slag would inhibit the diffusion of Ti^{4+} ions; i.e., the viscosity of the slag has an important effect on the diffusion of Ti^{4+} ions. In the present study, the viscosity of slags D, A, and E (basicity = 0.8, 1, and 1.2) calculated by Zhang's model [11–12] was 2.68, 2.14, and 1.08 Pa·s, respectively. From the viewpoint of viscosity, the thickness of the D–D layer should increase with increasing basicity. However, CaO could easily unite with TiO_2 in the dissolution layer to form $CaTiO_3$, which could precipitate from the slag; this outcome is shown in Figs. 2 and 3. The precipitation of $CaTiO_3$ would make the slag viscous and the dissolution rate slow; therefore, the thickness of the D–D layer in slag A was smaller than that in slag D. A comparison of the thickness of the D–D layer in slags D and E reveals that the effect of the formation of the $CaTiO_3$ phase on diffusion was more significant.

4.2. Estimation of Ti^{4+} diffusivity in molten slags

Because the diffusion of Ti^{4+} plays an important role during the dissolution process, an evaluation of its diffusion ability is necessary. To calculate the diffusivity of Ti^{4+} ions in a molten slag, the following assumptions are made: (1) the diffusion of Ti^{4+} toward a slag is unidirectional, semi-infinite diffusion; (2) The diffusivity of Ti^{4+} in a slag is constant.

On the basis of these two assumptions, the following solution to Fick's second law can be used to estimate the diffusivity of Ti^{4+} ions in the slag [6,13]:

$$\frac{c}{c_{ie}} = \mathrm{erfc}\left(\frac{x}{2\sqrt{Dt}}\right) \tag{1}$$

The initial and final boundary conditions are

$$\begin{cases} t = 0, x > l & c = 0 \\ t > 0, x = l & c = c_{ie} \end{cases} \tag{2}$$

where c_{ie} is the concentration of Ti^{4+} in the dissolution layer very close to the interface between the dissolution layer and slag, c is the concentration of Ti^{4+} at x, and l or x corresponds to the interface between the dissolution layer and slag. On the basis of the concentration profiles of Ti^{4+} in the dotted box in Fig. 4, we used Eq. (1) to calculate the diffusivities of Ti^{4+} ions in different slags; the results are shown in Table 2.

In molten slag, the relationship between the diffusivity of a diffusing species and viscosity can be expressed by the Stokes–Einstein relation [9,13]. According to this relation, the diffusivity (D) can be estimated by the viscosity (η) of the molten slag using the following equation:

$$D = \frac{kT}{6\pi r\eta} \quad (3)$$

where k is the Boltzmann constant, T is the absolute temperature, and r is the radius of the diffusing species. In the present study, the viscosity was calculated using Zhang's model [11–12], which has been used to successfully estimate the viscosity of aluminosilicate melts. Combining Eq. (3) and Zhang's model, we obtained the diffusivities of Ti^{4+} ions in different slags; the results are listed in Table 2.

The diffusivities of Ti^{4+} ions in the bulk slag plotted as a function of temperature, basicity, and Al_2O_3 content are shown in Fig. 6. A comparison of these two results reveals that temperature has the same effect on both diffusivities, whereas basicity and Al_2O_3 content have contrary effects. In addition, the diffusivity calculated from the viscosity is larger than that estimated using Eq. (1). Two plausible reasons can explain this discrepancy. First, because of high TiO_2 content and the formation of $CaTiO_3$, the mobility of the molten slag in the dissolution layer decreases, and this enhances the resistance to diffusion. Second, Ti^{4+} ions may act as a network former, and the they are always present as tetrahedral TiO_4^{4-} structures in molten slags [14–15]; therefore, setting the r term in Eq. (3) equal to the radius of a Ti^{4+} ion is inappropriate. Ukyo and Goto [16] investigated the interdiffusivities of TiO_2 in a liquid 40wt% CaO–40wt%SiO_2–Al_2O_3 slag and found that the interdiffusivity at 1673 K was 6.0×10^{-7} $cm^2 \cdot s^{-1}$. In their study, two kinds of liquid slags were used to prepare diffusion couples; hence, their results cannot be compared to results obtained in this work. Notably, however, the orders of magnitude of the results are very similar.

Table 2. Diffusivities of Ti^{4+} ions in bulk slags

Slag No.	Temperature / K	Diffusivity / ($cm^2 \cdot s^{-1}$)	
		Eq. (1)	Eq. (3)
A	1643	2.224×10^{-10}	8.744×10^{-8}
	1673	2.204×10^{-8}	9.435×10^{-8}
	1703	4.549×10^{-8}	1.357×10^{-7}
B	1673	1.885×10^{-8}	1.380×10^{-7}
C	1673	4.609×10^{-9}	9.113×10^{-7}
D	1673	1.161×10^{-7}	7.553×10^{-8}
E	1673	1.701×10^{-8}	1.869×10^{-7}

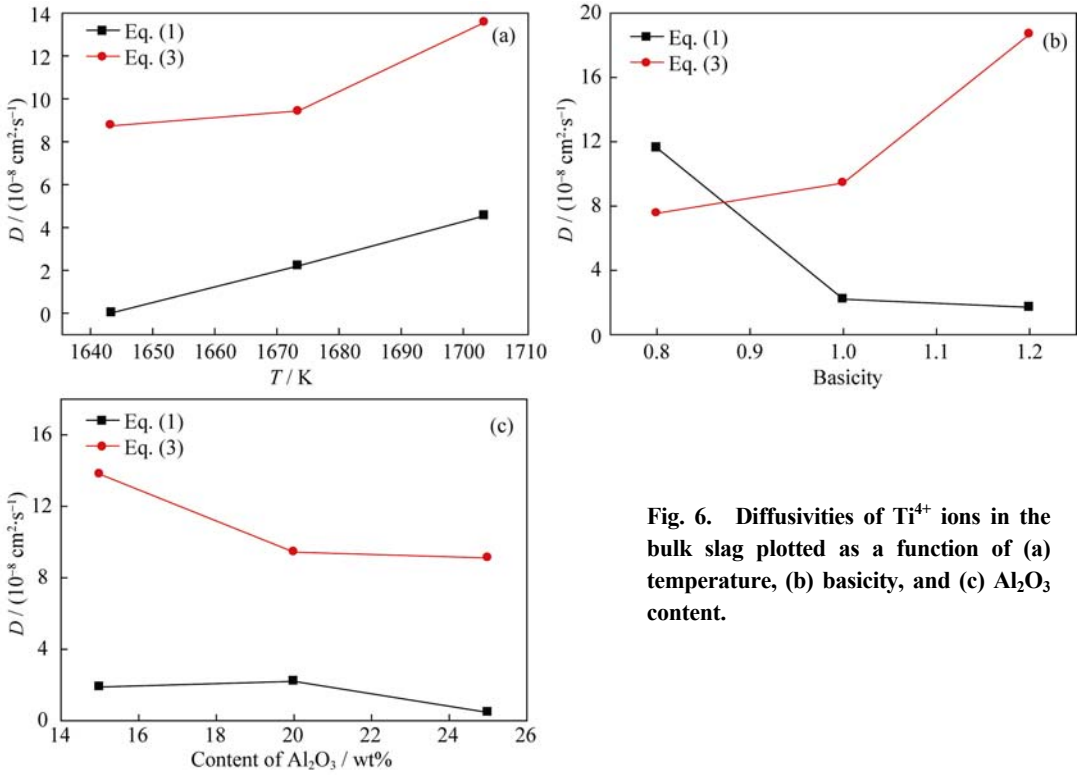

Fig. 6. Diffusivities of Ti^{4+} ions in the bulk slag plotted as a function of (a) temperature, (b) basicity, and (c) Al_2O_3 content.

4.3. Mechanism of dissolution of TiO_2 into slags

On the basis of the previous discussion, we here propose a reasonable mechanism of TiO_2 dissolution into slag. The mechanism of TiO_2 dissolution into the slag can be considered to consist of three stages, as illustrated in Fig. 7. In the first stage, TiO_2 diffuses toward the bulk slag, and the slag begins to erode TiO_2, as shown in Fig. 7(a). The TiO_2 dis-

solves in the second stage, where the dissolution rate is larger than the diffusion rate, which causes TiO_2 to accumulate in the dissolution layer and leads to an increase in TiO_2 content. The diffusion of Ti^{4+} ions, which occurs mainly in the dissolution layer, makes the composition of the dissolution layer homogeneous. In the third stage, because the solubility of TiO_2 is limited, the erosion of TiO_2 by the slag begins to become difficult when TiO_2 is abundant in the slag. Meanwhile, reactions between TiO_2 and CaO occur, leading to the precipitation of $CaTiO_3$ from the slag, as shown in Figs. 2 and 3.

Having elucidated the mechanism of TiO_2 dissolution into the slag, we can better understand the growth of the D–D layer. Because of a greater dissolution rate, the interfacial thickness sharply increased in the earlier stage. In the second stage, the increase in TiO_2 content in the bulk slag resulted in a greater viscosity. Moreover, the formation of $CaTiO_3$ enhanced the resistance to dissolution and diffusion, and thus the growth rate of the D–D layer decreased, as shown in Fig. 5(b).

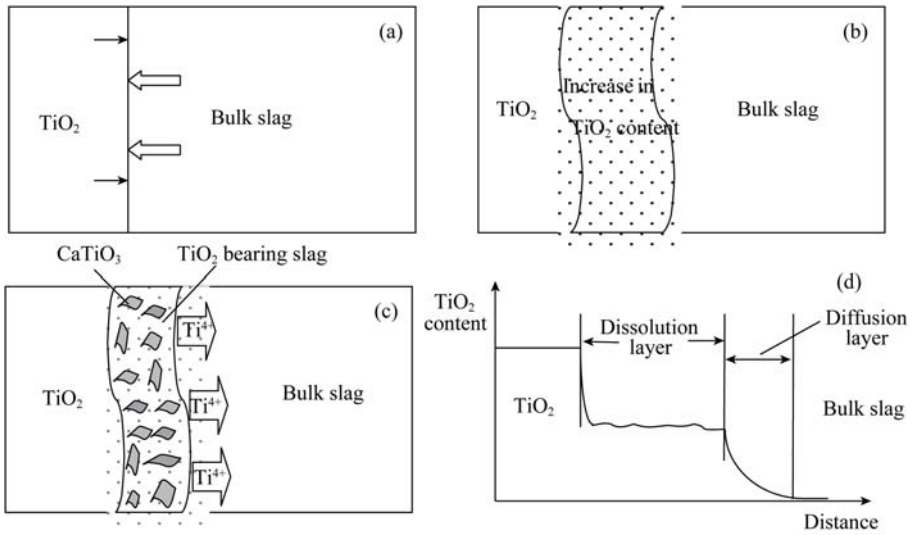

Fig. 7. Schematics of the dissolution mechanism and concentration profile of TiO_2 across the interface between TiO_2 and the slag.

5. Conclusions

The dissolution and diffusion behavior of TiO_2 in a molten CaO–Al_2O_3–SiO_2 slag at 1643–1703 K was investigated. The dissolution procedure of TiO_2 into the slag can be divided into three stages. In the first two stages, the dissolution of TiO_2 was rapid, along with the diffusion of Ti^{4+} into the dissolution layer. In the third stage, the $CaTiO_3$ phase began to precipitate due to the local higher TiO_2 concentration in the dissolution layer, and the dissolution rate was mainly controlled by the diffusion of Ti^{4+} ions toward the bulk slag. Higher temperatures favored the dissolution and diffusion of TiO_2, whereas a greater Al_2O_3 content in the slag restrained the dissolution and diffusion. With increasing basicity, the thickness of the D–D layer first decreased and then increased. In addition, the effect of the formation of $CaTiO_3$ on diffusion was more important. The diffusivities of Ti^{4+} ions in the bulk slags were estimated from the concentration profiles of Ti and were lower than those calculated according to the Stokes–Einstein relation. The orders of magnitude of the diffusivities were in the range of 10^{-10}–10^{-7} $cm^2 \cdot s^{-1}$.

Acknowledgements

The financial support from the National Science Foundation of China (No. 51090384) is gratefully acknowledged.

References

[1] M. Wang, Y.P. Bao, H. Cui, H.J. Wu, and W.S. Wu, Generation mechanism of Al_2O_3–TiN inclusion in IF steel, *J. Iron Steel Res.*, 22(2010), No. 7, p. 29.

[2] A.O. Kluken and Ø. Grong, Mechanisms of inclusion formation in Al–Ti–Si–Mn deoxidized steel weld metals, *Metall. Trans. A*, 20(1989), No. 8, p. 1335.

[3] W.C. Doo, D.Y. Kim, S.C. Kang, and K.W. Yi, The morphology of Al–Ti–O complex oxide inclusions formed in an ultra low-carbon steel melt during the RH process, *Met. Mater. Int.*, 13(2007), No. 3, p. 249.

[4] M.K. Sun, I.H. Jung, and H.G. Lee, Morphology and chemistry of oxide inclusions after Al and Ti complex deoxidation, *Met. Mater. Int.*, 14(2008), No. 6, p. 791.

[5] R.F. Johnston, R.A. Stark, and J. Taylor, Diffusion in liquid slags, *Ironmaking Steelmaking*, 4(1974), p. 220.

[6] Z. Ping and S. Seetharaman, Dissolution of MgO in CaO–"FeO"–CaF_2–SiO_2 slags under static conditions, *J. Am.*

Ceram. Soc., 77(1994), No. 4, p. 970.

[7] S.H. Amini, M.P. Brungs, S. Jahanshahi, and O. Ostrovski, Effects of additives and temperature on dissolution rate and diffusivity of lime in Al_2O_3–CaO–SiO_2 based slags, *Metall. Mater. Trans. B*, 37(2006), p. 773.

[8] J.H. Park, I.H. Jung, and H.G. Lee, Dissolution behavior of Al_2O_3 and MgO inclusions in the CaO–Al_2O_3–SiO_2 slags: formation of ring-like structure of $MgAl_2O_4$ and Ca_2SiO_4 around MgO inclusions, *ISIJ Int.*, 46(2006), No. 11, p. 1626.

[9] X. Yu, R.J. Pomfret, and K.S. Coley, Dissolution of alumina in mold fluxes, *Metall. Mater. Trans. B*, 28(1997), No. 2, p. 275.

[10] D.Y. Wang, J. Liu, M.F. Jang, F. Tsukihashi, and H. Matsuura, Dissolution of Al_2TiO_5 inclusions in CaO–SiO_2–Al_2O_3 slags at 1823 K, *Int. J. Miner. Met. Mater.*, 18(2011), No. 6, p. 646.

[11] G.H. Zhang and K.C. Chou, Modeling the viscosity of alumino-silicate melt, *Steel Res. Int.*, 84(2013), No. 7, p. 631.

[12] G.H. Zhang, K.C. Chou, and K. Mills, Modelling viscosities of CaO–MgO–Al_2O_3–SiO_2 molten slags, *ISIJ Int.*, 52(2012), No. 3, p. 355.

[13] M.D. Dolan and R.F. Johnston, Multicomponent diffusion in molten slags, *Metall. Mater. Trans. B*, 35(2004), No. 4, p. 675.

[14] *Slag Atlas*, 2nd Ed., Edited by VDEh, Verlag Sthaleisen GmbH, Germany, 1995, p. 6.

[15] Z. Wang, Q.F. Shu, and K.C. Chou, Structure of CaO–B_2O_3–SiO_2–TiO_2 glasses: a Raman spectral study, *ISIJ Int.*, 51(2011), No. 7, p. 1021.

[16] Y. Ukyo and K.S. Goto, Measurement of quasi-binary interdiffusivities of various oxides in liquid slags, *Tetsu-to-Hagane*, 68(1982), No. 14, p. 1981.